Nonoscillatory Forward-in-time differencing for fluids: simulation of global solar dynamo

Piotr K. Smolarkiewicz

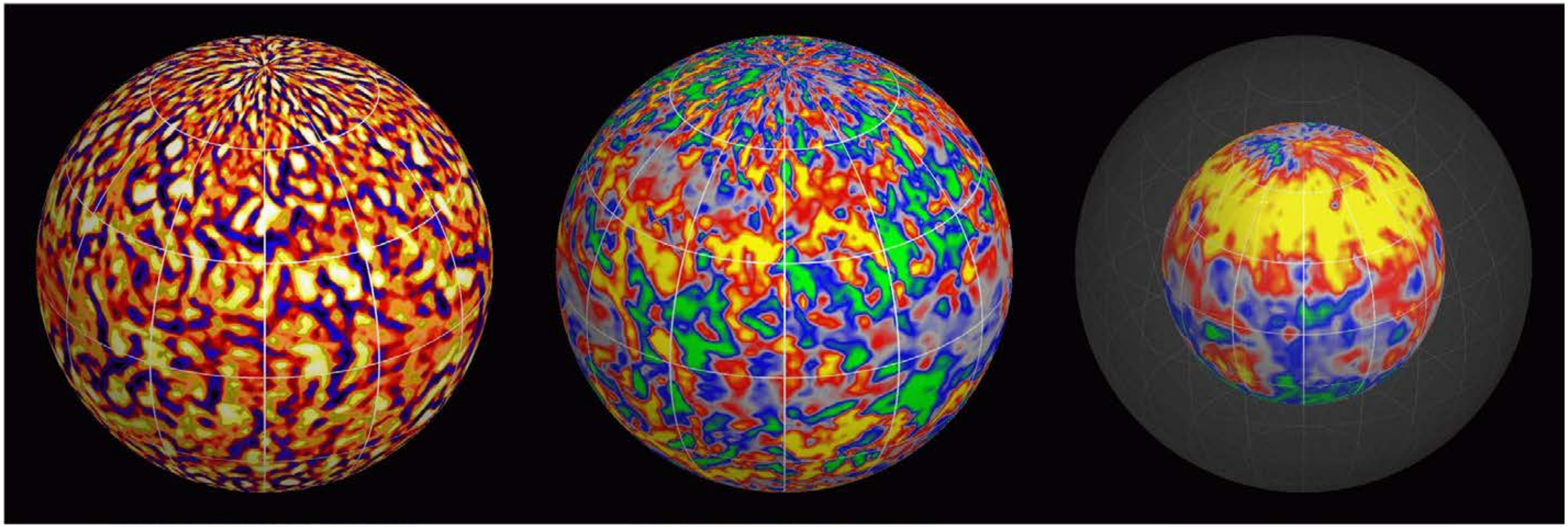

European Research Council
Established by the European Commission
Supporting top researchers from anywhere in the world

Earlier experience with self-organization includes “virtual-labs” for QBO (**dns**), MJO (**iles**), and evolutionary sand dunes (**les**); with overall role of explicit SGS closures being mostly catalytic.

RE: SGS Modeling vs Filtering

- The importance of "physical" role of SGS modeling and filtering may be overstated while their mathematical role (L^2 integrability) may be underappreciated.

- Universal SGS modeling or filtering may not exist, as the models and filters appear to be problem & numerics dependent. The majority of known SGS models/filters targets centered in time-and-space numerics.

- Successful simulation of self organization and the emergence of coherent structures in time-space continuum seems to depend on handling the entire chain of events, so it may not be reducible to a SGS modeling/filtering issue.

Relevant aspects of numerics:

A suit of governing PDEs, including anelastic solar MHD as a special application.

Nonoscillatory Forward in Time (NFT) semi-implicit model integration algorithms (finite-volume or semi-Lagrangian, and symplectic representation of key physical forcings.

Robust elliptic solver, inverting full stiff boundary-value problems to a round-off error accuracy (viz. exact projection).

Tensor formalism underlies numerical model, enabling static and dynamic grid stretching with uniformly 2nd order accuracy.

Explicit SGS models available, but most calculations relies on ILES property of MPDATA

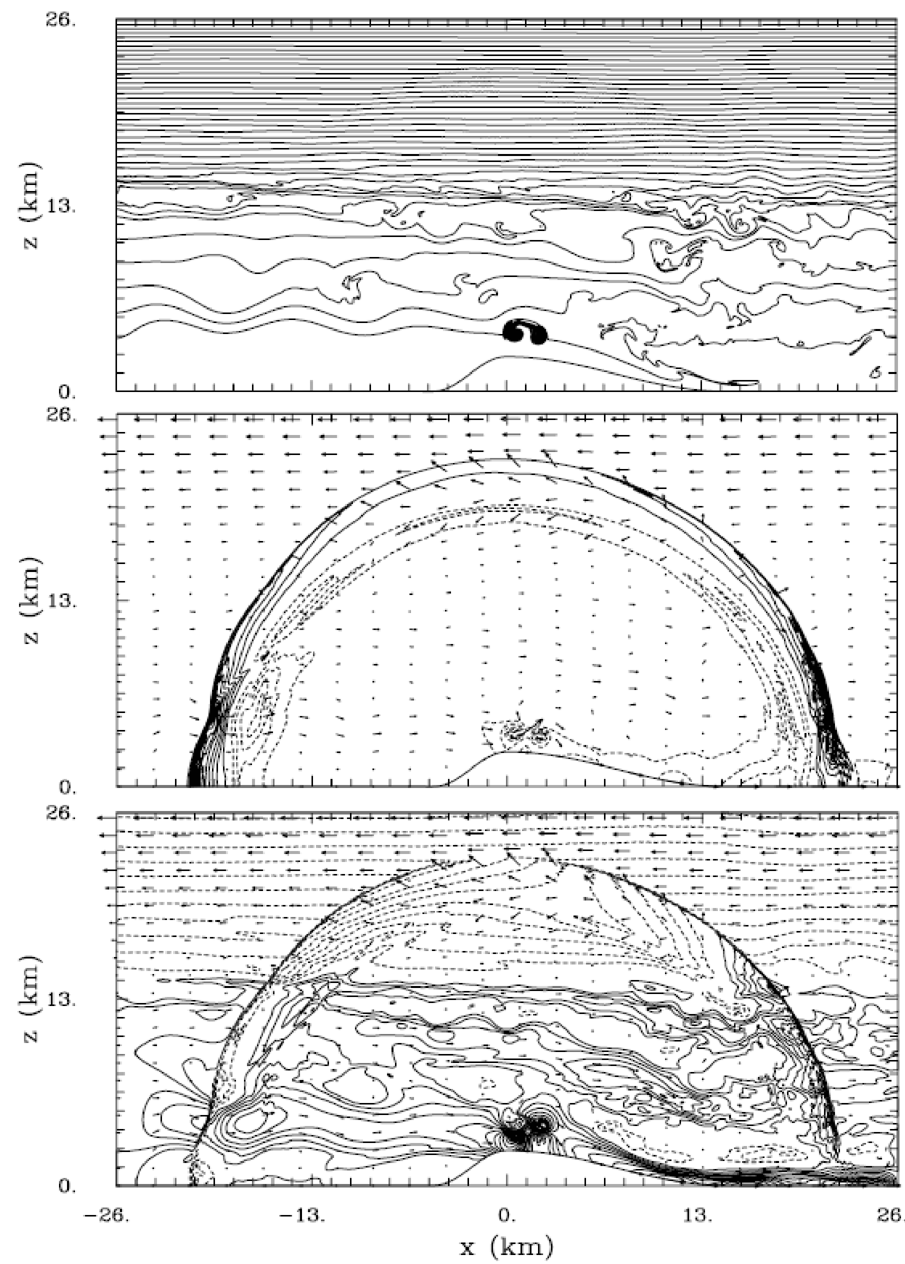

An elemental solar MHD formulation in EULAG

$$\frac{d\mathbf{u}}{dt} = -\nabla\pi' - \mathbf{g}\frac{\Theta'}{\Theta_o} + 2\mathbf{u}\times\mathbf{\Omega} + \frac{1}{\mu\rho_o}\mathbf{B}\cdot\nabla\mathbf{B} \ ,$$

$$\frac{d\Theta'}{dt} = -\mathbf{u}\cdot\nabla\Theta_e + \frac{1}{\rho_o}\mathcal{H}(\Theta') - \alpha\Theta' \ ,$$

$$\frac{d\mathbf{B}}{dt} = \mathbf{B}\cdot\nabla\mathbf{u} - \mathbf{B}\nabla\cdot\mathbf{u} \ ,$$

$$\nabla\cdot\rho_o\mathbf{u} = 0 \ ,$$

$$\nabla\cdot\mathbf{B} = 0 \ .$$

The underlying ambient state assumes mean Sun

$$0 = -\frac{\partial}{\partial r}\left(\frac{p_e - p_o}{\rho_o}\right) + g\frac{\Theta_e - \Theta_o}{\Theta_o} \ ,$$

$$0 = \mathcal{H}(\Theta_e) + \mathcal{H}^* \ ,$$

Numerical framework:

$$\frac{\partial \rho^* \Psi}{\partial \overline{t}} + \overline{\overline{\nabla}} \cdot (\mathbf{V}^* \Psi) = \rho^* \mathbf{R} \ ,$$

$$\Psi = \{\mathbf{u}, \Theta', \mathbf{B}\}^T$$

$$\mathbf{R} = \{\mathbf{R_u}, R_{\Theta'}, \mathbf{R_B}\}^T$$

$$\boxed{\overline{\mathbf{B}}^* \cdot \overline{\nabla} \mathbf{B} = \frac{1}{\overline{\overline{\mathcal{G}}}} \overline{\nabla} \cdot \overline{\mathcal{G}} \, \overline{\mathbf{B}}^* \mathbf{B} \ , \quad \overline{\mathbf{B}}^* \cdot \overline{\nabla} \mathbf{u} = \frac{1}{\overline{\overline{\mathcal{G}}}} \overline{\nabla} \cdot \overline{\mathcal{G}} \, \overline{\mathbf{B}}^* \mathbf{u}}$$

$$\Psi_{\rm i}^n = \mathcal{A}_{\rm i}\left(\widetilde{\Psi}, \, \widetilde{\mathbf{V}}^*, \, \rho^*\right) + 0.5\delta t \mathbf{R}_{\rm i}^n \equiv \widehat{\Psi}_{\rm i} + 0.5\delta t \mathbf{R}_{\rm i}^n$$

$$\Psi_{\rm i}^{n,\nu} = \widehat{\Psi}_{\rm i} + 0.5\delta t \ \mathbf{L}\Psi\big|_{\rm i}^{n,\nu} + 0.5\delta t \ \mathbf{N}(\Psi)\big|_{\rm i}^{n,\nu-1} - 0.5\delta t \ \widetilde{\mathbf{G}}\overline{\nabla}\Phi\big|_{\rm i}^{n,\nu}$$

$$\boxed{\Phi \equiv (\pi', \ \pi', \ \pi', \ 0, \ \pi^*, \ \pi^*, \ \pi^*)}$$

$$\Psi_{\rm i}^{n,\nu} = [\mathbf{I} - 0.5\delta t \mathbf{L}]^{-1}\left(\widehat{\widehat{\Psi}} - 0.5\delta t \widetilde{\mathbf{G}}\overline{\nabla}\Phi^{n,\nu}\right)\Big|_{\rm i}$$

$$\widehat{\widehat{\Psi}} \equiv \widehat{\Psi} + 0.5\delta t \mathbf{N}\Psi\big|^{n,\nu-1}$$

➔ elliptic problems for potentials Φ

Power of ILES; L^2 integrability

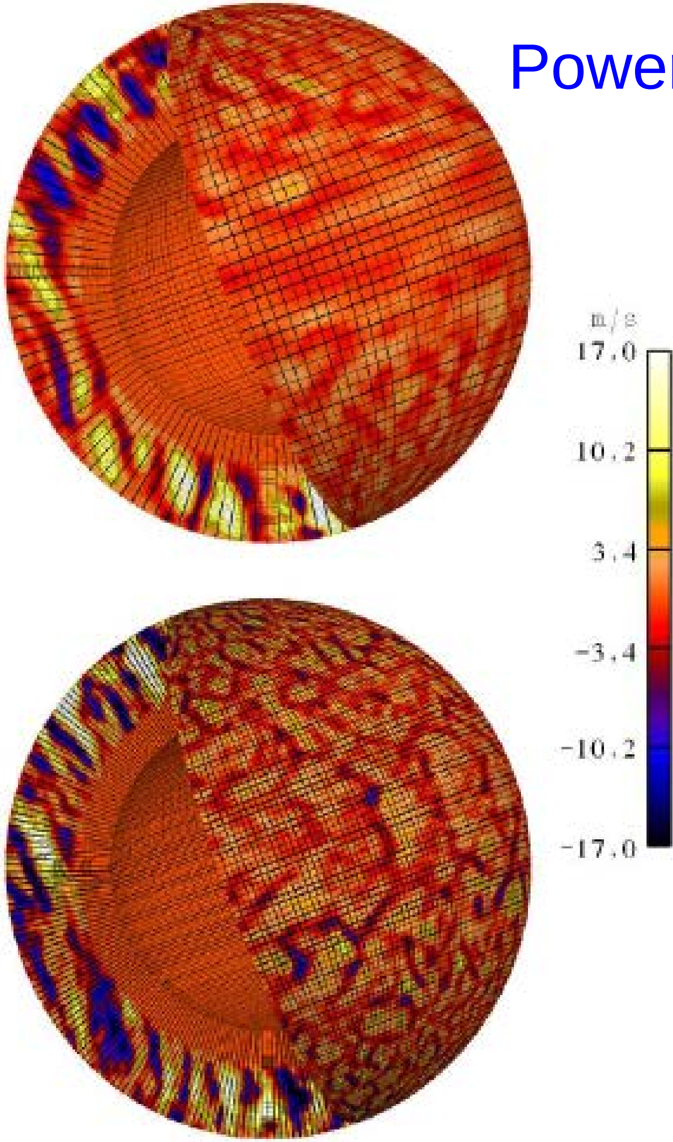

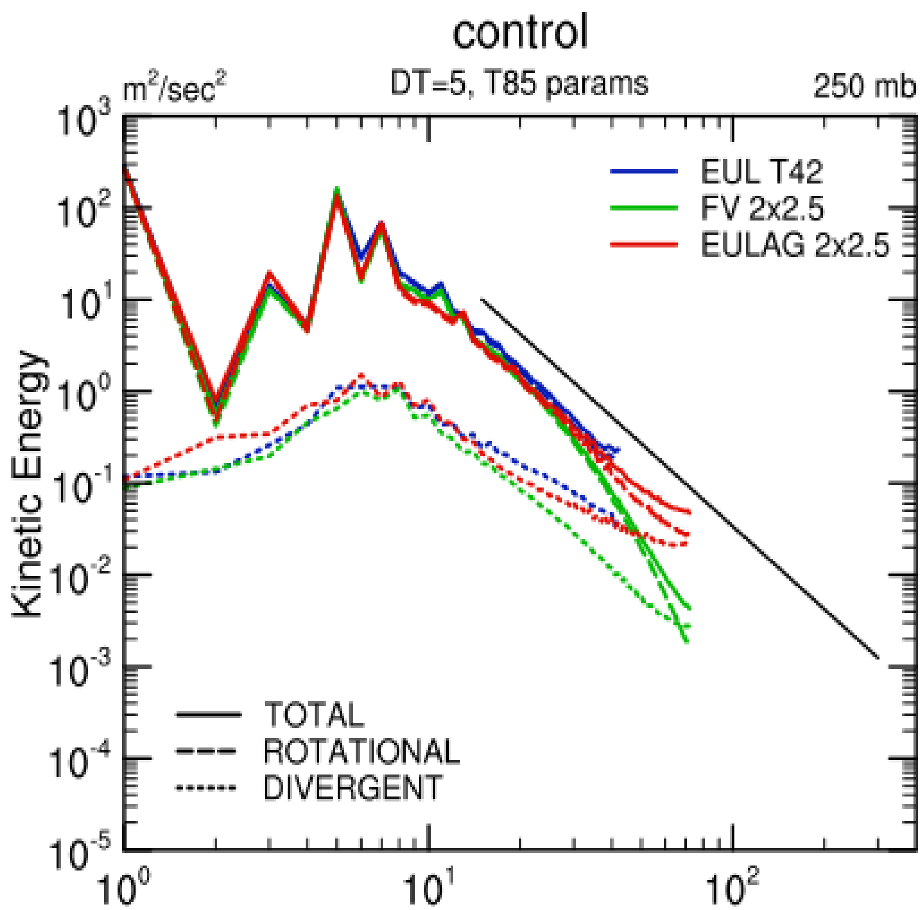

Fig. 1. Color rendering of the radial component of the flow velocity in two simulations carried out on a longitude-latitude-radius spatial mesh of size $128 \times 64 \times 47$ (top) and $256 \times 128 \times 96$ (bottom), with the mesh lines overlaid as black lines. Both snapshots are taken many tens of convective eddy turnover times after convection has reached a statistically stationary state. The tendencies for convective flow structures to align themselves parallel to the rotation axis at low latitudes is typical of global simulations of solar convection, with or without magnetic fields, operating in this parameter regime (see, e.g., Fig. 1 in [6]; Fig. 2 in [28]).

Mode of large-scale dynamo action

$$\mathbf{u}'(r,\theta,\phi,t) = \mathbf{u}(r,\theta,\phi,t) - \langle\mathbf{u}\rangle(r,\theta,t)$$
$$\mathbf{B}'(r,\theta,\phi,t) = \mathbf{B}(r,\theta,\phi,t) - \langle\mathbf{B}\rangle(r,\theta,t)$$

$$\frac{\partial\langle\mathbf{B}\rangle}{\partial t} = \nabla\times\langle\mathbf{u}\rangle\times\langle\mathbf{B}\rangle + \nabla\times\langle\mathbf{u}'\times\mathbf{B}'\rangle$$

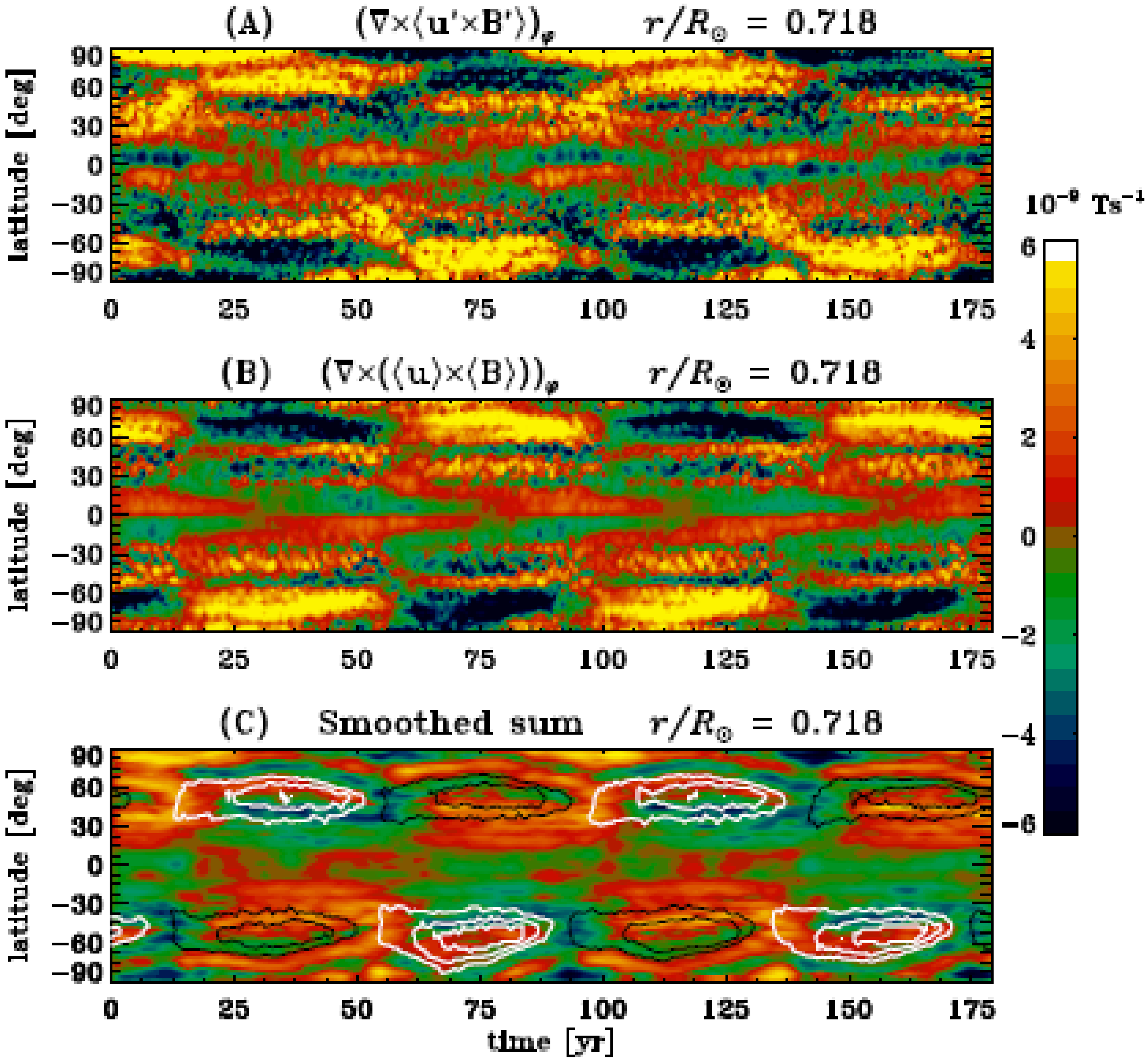

Fig. 5. The two inductive contributions to the zonally-averaged large-scale zonal magnetic component, for the same simulation and over the same time interval as in Fig. 4. (A) induction by the turbulent electromotive force; (B) Induction by the large scale flow; (C) the sum of the above two on the same color scale, with a few isocontours of mean zonal field overplotted (black/white for negative/positive).

Acknowledgements

European Research Council
Established by the European Commission
Supporting top researchers from anywhere in the world

EULAG-MHD offers a unique virtual laboratory for addressing questions on numerics, mathematics and physics underlying simulation of solar MHD

This work has received funding from the European Research Council under the EU's Seventh Framework Programme (FP7/2012/ERC Grant agreement no. 320375)